Ellipsoidal Shell Subtraction Model of Right Ventricular Volume

Comparison With Regional Free Wall Dimensions as Indexes of Right Ventricular Function

Michael P. Feneley, Joseph R. Elbeery, J. William Gaynor, Stanley A. Gall Jr., James W. Davis, and J. Scott Rankin

Pulse–transit sonomicrometry was used to measure the base–apex (a), anteroposterior (b), and septal–free wall (c) diameters of the left ventricle and the septal–free wall diameter of the right ventricle (d) in eight excised and three isolated, pump-perfused canine heart preparations, as well as in nine conscious dogs. In the three perfused hearts and in four of the excised hearts, right ventricular free wall regional segment lengths and segment area also were assessed. Biventricular volumes were measured directly with intracavitary balloons in all isolated hearts. When left ventricular balloon volume was held constant, relations between right ventricular free wall dimensions and right ventricular balloon volume were highly linear. With increments in left ventricular volume, however, these relations remained linear but shifted progressively upward, indicating an independent relation between right ventricular free wall dimensions and left ventricular cavitary volume. An ellipsoidal shell subtraction model ($\pi/6 \cdot$ abd minus right ventricular free wall volume) was developed to estimate right ventricular cavitary volume from cardiac dimensions. With this method, a highly linear relation was observed between calculated right ventricular volume and right ventricular balloon volume (mean $r=0.99\pm0.01$). Moreover, this relation appeared to be independent of changes in left ventricular balloon volume. With the shell subtraction model, dynamic right ventricular volume was computed in nine conscious dogs, and in four, stroke volume derived from dimensions was compared with right ventricular stroke volume measured with ultrasonic flow probes. A highly linear relation was observed, suggesting the accuracy of the shell subtraction method in vivo. Right ventricular end-systolic pressure–volume and stroke work/end-diastolic volume relations then were evaluated, and both proved to be highly linear in the right ventricle (both mean $r=0.99\pm0.01$). Thus, the shell subtraction model allows a simple estimate of dynamic right ventricular volume in the intact heart and facilitates assessment of right ventricular performance in vivo. (*Circulation Research* 1990;67:1427–1436)

When compared with current knowledge of left ventricular function, knowledge concerning the performance characteristics of the right ventricle, particularly in vivo, is small. The lack of an accurate method for determining instantaneous right ventricular volume in the intact heart is the major reason for this discrepancy. Estimation of dynamic left ventricular volume now is possible in conscious dogs by applying an ellipsoidal geometric algorithm to left ventricular dimensions measured continuously with implanted ultrasonic transducers.[1–4] Because of the more complex geometry of the right ventricle, however, an algorithm permitting derivation of right ventricular volume from continuous measurements of right ventricular dimensions has not been practical.

Some investigators have tried to circumvent this limitation by using measurements of right ventricular regional dimensions as indexes of changes in right ventricular volume.[5–7] But problems may exist with this approach because of the well-documented interactive effects of left ventricular volume on right ventricular shape.[2,8] One even could hypothesize that the relation between right ventricular dimensions and volume might be influenced to a significant degree by changes in left ventricular volume. How-

From the Department of Surgery, Duke University Medical Center, Durham, N.C., and the Division of Cardiothoracic Surgery, University of California, San Francisco, San Francisco, Calif.

Supported by National Institutes of Health grants HL-09315, HL-29436, and HL-06607.

Address for correspondence: J. Scott Rankin, MD, 505 Parnassus Ave., Room M593, San Francisco, CA 94143-0118.

Received August 15, 1989; accepted August 2, 1990.

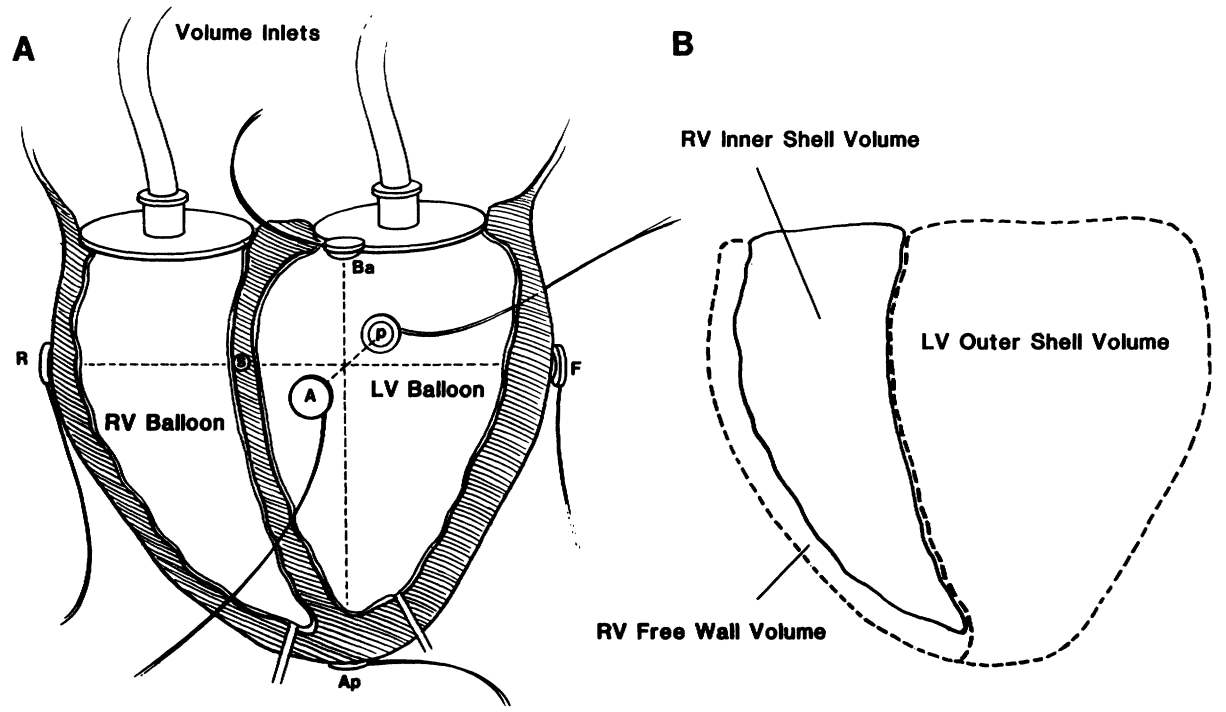

FIGURE 1. Panel A: *Illustration of the isolated heart preparation, showing left and right ventricular latex balloons and orthogonal arrays of ultrasonic dimension transducers. Ba–Ap is the major axis diameter (diameter a), A–p is the anteroposterior minor axis diameter (diameter b), s–F is the left ventricular septal–free wall diameter (diameter c), and s–R is the right ventricular septal–free wall diameter (diameter d).* Panel B: *Illustration of the ellipsoidal shell subtraction model. The volume within the right ventricular (RV) cavity is obtained by subtracting the left ventricular (LV) outer shell volume together with the right ventricular free wall volume from the total biventricular shell volume.*

ever, knowledge of the potential effects of left ventricular volume on right ventricular geometry is incomplete at present.

The first purpose of this study was to examine the independent relation between right ventricular regional dimensions and the volumes of both the right and left ventricles. The second purpose was to develop a method for derivation of right ventricular volume from ultrasonic cardiac dimension measurements using a geometric algorithm that was insensitive to changes in right ventricular cavity shape caused by changes in left ventricular volume. The third purpose was to assess the potential utility of this right ventricular volume algorithm in evaluating right ventricular function in vivo.

Materials and Methods

Isolated Heart Studies

Experimental preparation. Under general anesthesia with intravenous thiamylal sodium (30 mg/kg) and while being ventilated with a Harvard respirator (Harvard Apparatus, South Natick, Mass.), the hearts of 11 healthy, adult dogs (19–25 kg) were exposed through a left thoracotomy. In eight of the dogs, the heart was excised after being arrested by intravenous injection of potassium chloride (30 meq). In the remaining three dogs, the beating heart was isolated and removed to a blood reservoir. Coronary perfusion was established into an aortic root cannula using a roller pump, blood warmer, and oxygenator. Small vents were placed into the apexes of both ventricles. Coronary arterial pressure, monitored with a micromanometer (model MPC-500, Millar Instruments, Houston) in the aortic root, was maintained at 80–100 mm Hg, and blood temperature was kept at 37° C.

In each of the 11 isolated hearts, pulse–transit ultrasonic dimension transducers were positioned across the base–apex major axis and anteroposterior minor axis diameters of the left ventricle, and also across the septal–free wall minor axis diameters of both the left and right ventricles (Figure 1A). The positioning of this orthogonal array of transducers has been described in detail previously.[2,8]

In the three isolated, perfused hearts and in four of the eight arrested hearts, an additional orthogonal array of two pairs of regional cylindrical crystals (1.5 mm o.d.) was positioned in the subepicardial midportion of the right ventricular free wall. One pair of transducers was positioned parallel, and the other perpendicular, to the major axis diameter to measure long-axis and short-axis free wall segment length, respectively.

In all 11 hearts, both atria were opened widely, the mitral and tricuspid valves were excised, and thin high-volume compliant balloons attached to plastic sewing rings were inserted into both ventricles (Figure 1A). The sewing rings were sutured to the mitral

and tricuspid valve annuli. The pulmonary valves of all hearts and the aortic valves of the arrested hearts were sutured closed to prevent prolapse of the ventricular balloons during inflation. In the three perfused hearts, prolapse of the left ventricular balloon into the aorta was prevented by a flange on the mitral sewing ring that extended under the aortic valve. The space between the balloons and the ventricular walls was minimized in the perfused hearts by applying gentle suction to the ventricular vents throughout the experiments.

The three perfused hearts were studied while suspended in air with the apex dependent. To minimize possible gravitational distortions of ventricular geometry, the more flaccid arrested hearts were suspended in a warm isotonic saline bath during data acquisition.

Data acquisition and experimental protocol. Descriptions of the operating characteristics of the data acquisition hardware have been given in previous reports.[2,3,9] The ultrasonic dimension transducers were coupled to a sonomicrometer designed and built in our laboratory. Dimensional data were recorded at multiple, steady-state levels of right and left ventricular balloon volumes, which were varied independently over a wide range (0–60 ml, depending on heart size) by injection of normal saline in increments of 10 ml. After completion of data collection, the right ventricular free wall was trimmed from the left ventricle, and the volume of each was determined by water displacement.

Data analysis. Analog data were digitized in real time at 200 Hz (model 1012 A/D converter, ADAC, Woburn, Mass.) and analyzed on a microprocessor (model PDP 11/23, Digital Equipment Corp., Marlboro, Mass.). The volume of the right ventricular chamber was calculated from the ultrasonic cardiac dimension measurements according to an ellipsoidal shell subtraction model, the principle of which is illustrated in Figure 1B. Inspection of this figure shows that the total volume within the epicardial (outer) shell of both ventricles, which will be called the biventricular epicardial shell volume (BVV_{epi}), is equivalent to the sum of the left ventricular epicardial (outer) shell volume (LVV_{epi}), the volume within the endocardial (inner) shell of the right ventricle (RVV_{endo}), and the volume of the right ventricular free wall (FWV):

$$BVV_{epi}=LVV_{epi}+RVV_{endo}+FWV \quad (1)$$

Rearrangement of Equation 1 yields

$$RVV_{endo}=BVV_{epi}-LVV_{epi}-FWV \quad (2)$$

Equation 2 is the general equation of the shell subtraction model, according to which right ventricular cavity volume can be calculated by subtracting the outer shell volume of the left ventricle and right ventricular free wall volume from the outer biventricular shell volume.

Inspection of Figure 1B suggests also that the shapes of the biventricular outer shell and the left ventricular outer shell are similar and might be described as truncated ellipsoids. We have demonstrated previously,[2,10] however, that an accurate index of LVV_{epi} may be obtained by fitting the three epicardial major and minor axial dimensions of the left ventricle shown in Figure 1A (see diameters a, b, and c in figure legend) to the simpler formula for a general ellipsoid with major radius a/2 and minor radii b/2 and c/2:

$$LVV_{epi}=\frac{4\pi}{3}\frac{a}{2}\cdot\frac{b}{2}\cdot\frac{c}{2}=\frac{\pi}{6}a\cdot b\cdot c \quad (3)$$

A more detailed explanation of the derivation of Equation 3 is provided in Appendix A of Reference 2.

The similar shape of the biventricular outer shell led us to postulate that BVV_{epi} also might be estimated by fitting its three epicardial major and minor axial dimensions to the formula for a general ellipsoid. The base–apex dimension (dimension a) and anteroposterior dimension (dimension b) are common to both the biventricular and left ventricular outer shells (Figure 1A), but the third axial dimension of the biventricular outer shell is equal to the sum of the septal–free wall dimensions of both ventricles (dimension c+d). Fitting these three axial dimensions of the biventricular outer shell to the formula for a general ellipsoid with major radius a/2 and minor radii b/2 and (c+d)/2 yields the following formula for BVV_{epi}:

$$BVV_{epi}=\frac{4\pi}{3}\frac{a}{2}\cdot\frac{b}{2}\cdot\frac{(c+d)}{2}=\frac{\pi}{6}a\cdot b\cdot(c+d) \quad (4)$$

Substitution of Equations 3 and 4 for LVV_{epi} and BVV_{epi} in Equation 2 yields

$$RVV_{endo}=\frac{\pi}{6}a\cdot b\cdot(c+d)-\frac{\pi}{6}a\cdot b\cdot c-FWV \quad (5)$$

$$=\frac{\pi}{6}a\cdot b\cdot d-FWV$$

At each steady-state level of left and right ventricular balloon volumes, right ventricular chamber volume was calculated with Equation 5. In addition, the product of the orthogonal long-axis and short-axis right ventricular free wall regional segment lengths was calculated to measure right ventricular free wall segment area. To ascertain the independent effects of changes in both right and left ventricular volumes on each of the right ventricular dimensions (right ventricular free wall segment lengths, segment area, and right ventricular septal–free wall diameter), multiple linear regression analyses were performed in which each of the right ventricular dimensions was treated as the dependent variable, and right and left ventricular balloon volumes were treated as the independent variables. Because free wall segment lengths and segment areas were measured in different units, all free wall dimensions were expressed

as percent changes from control values to facilitate comparison of their relations with ventricular volumes. The control values were defined as the ventricular dimensions observed when the balloons in both ventricles were completely deflated to zero distending pressure. The relations between right ventricular volume calculated with Equation 5 (dependent variable) and right and left ventricular balloon volumes (independent variables) were determined also by multiple linear regression analyses.

In Vivo Studies

Experimental preparation. Nine healthy adult dogs (19–26 kg) were anesthetized (thiamylal sodium 25 mg/kg i.v. and succinylcholine 1 mg/kg i.v.), intubated, and ventilated with a volume respirator (model MA1, Bennett, Los Angeles). A left thoracotomy was performed through the fifth intercostal space, and pulse–transit ultrasonic dimension transducers were positioned in the same biventricular orthogonal array described above for the isolated heart studies (Figure 1A).[2,8] Silicone rubber pneumatic occluders were positioned around both venae cavae. Heparin-filled silicone catheters (2.6 mm i.d.) were secured in the base of the left atrium and the apex of the right ventricle. The pericardium was left widely open. An ultrasonic transit–time flow probe (Transonic Systems, Inc., Ithaca, N.Y.) was positioned on the main pulmonary artery in four dogs.

Another silicone catheter with multiple side holes was positioned in the pleural space adjacent to the ventricular epicardium. The transducer leads, catheters, and occluder tubing were tunneled into a subcutaneous pouch dorsal to the thoracotomy, which was repaired in multiple layers. Procaine penicillin G (600,000 units i.m.) and dihydrostreptomycin (25 mg i.m.) were administered for 5 days postoperatively. After a recovery period of 7–14 days, the hardware was exteriorized from the subcutaneous pouch through a small skin incision under 1% lidocaine local anesthesia. Each animal was studied in the conscious state, lying quietly on its right side, 1 hour after light sedation (morphine sulfate, 5 mg i.m.).

Data acquisition and experimental protocol. The ultrasonic dimension transducers were coupled to the sonomicrometer, and the pulmonary artery flow probe was connected to an ultrasonic transit–time flowmeter (Transonic Systems). Micromanometer-tipped catheters (Millar, model MPC-500), which had been balanced and calibrated simultaneously to a water column, were passed via the implanted silicone catheters to obtain left ventricular, right ventricular, and pleural pressures in the closed-chest state. Pharmacological attenuation of autonomic reflexes was achieved by intravenous administration of propranolol (1 mg/kg) and atropine (0.4 mg/kg). Data were recorded under control conditions, during several transient complete vena caval occlusions, and during multiple levels of steady-state vena caval occlusion.

At the conclusion of the study, each animal was killed by intravenous injection of potassium chloride under deep barbiturate anesthesia. The heart was excised, and the satisfactory position of implanted hardware was confirmed. After excision of the atria and valve tissue, the right ventricular free wall was separated from the left ventricle, and the volume of each was determined by water displacement.

Data analysis. Analog data were digitized and analyzed with a microprocessor in the same manner as described for isolated heart studies. Left ventricular chamber volume was determined by subtracting measured left ventricular wall volume from the epicardial shell volume calculated with Equation 3.[2,3] Right ventricular chamber volume was computed with Equation 5. Left and right ventricular transmural pressures were calculated as the difference between the respective chamber pressures and pleural pressure. Measured right ventricular stroke volume was determined under control conditions and during each level of steady-state vena caval occlusion as the time integral of pulmonary artery flow. Calculated right ventricular stroke volume was derived as the change in right ventricular dimensional volume determined with Equation 5 over the same time period. The relation between calculated and measured right ventricular stroke volume was determined by linear regression analysis in four studies.

To evaluate the potential utility of the right ventricular volume algorithm in assessing right ventricular function in vivo, data recorded during transient vena caval occlusion were used to examine the relation between right ventricular stroke work and end-diastolic volume,[3] and also between end-systolic pressure and volume. End-systole was defined as the time of maximal elastance (pressure/volume ratio) during each cardiac cycle. Stroke work (SW) was calculated as the integral of ventricular transmural pressure (P) and calculated chamber volume (V):

$$SW = \int P \cdot dV \tag{6}$$

The relation between stroke work and end-diastolic volume (EDV) and the relation between end-systolic pressure (ESP) and end-systolic volume (ESV) were determined by linear regression analysis, according to the following equations:

$$SW = M_w (EDV - V_w) \tag{7}$$

$$ESP = E_{ES} (ESV - V_o) \tag{8}$$

where M_w and E_{ES} are the slopes, and V_w and V_o are the volume-axis intercepts of the stroke work/end-diastolic volume and end-systolic pressure–volume relation, respectively.

To evaluate the appropriateness of linear regression, multiple nonlinear regression analyses also were used to determine the values of the parameters A_s, B_s, C_s and A_p, B_p, C_p in the following equations

TABLE 1. Linear Regression of Right Ventricular Free Wall Dimensions Versus Right Ventricular Balloon Volume

Dimension	Linear correlation coefficient*		Slope (% change/ml)	
	vs. RVV	vs. LVV	vs. RVV	vs. LVV
Long-axis	0.96±0.05	0.95±0.04	0.40±0.21	0.16±0.10
Short-axis	0.97±0.04	0.97±0.02	0.52±0.21	0.17±0.07
Area	0.98±0.03	0.98±0.03	1.03±0.40	0.33±0.21

All dimensions were normalized as percent changes from control values (see "Materials and Methods"). RVV, right ventricular balloon volume; LVV, left ventricular balloon volume.
*All $p<0.01$.

that provided the best least-squares fit to each data set[11]:

$$SW=A_s\,EDV^2+B_s\,EDV+C_s \quad (9)$$

$$ESP=A_p\,ESV^2+B_p\,ESV+C_p \quad (10)$$

In these equations, the values of A_s and A_p indicate the curvilinearity of the respective relations. Positive and negative values indicate convexity and concavity toward the volume axis, respectively, whereas a value of zero indicates a linear relation. Whether A_s or A_p differed significantly from zero was determined with Student's t test, with the level of statistical significance set at $p<0.05$.

If A_s proved to be significantly different from zero, a nonlinear determination of the volume-axis intercept, V_w, also was made by solving Equation 9 for EDV when SW was set equal to zero, according to the quadratic formula

$$V_w=[-B_s+(B_s^2-4\,A_s\,C_s)^{1/2}]/2A_s \quad (11)$$

Similarly, if A_p proved to be significantly different from zero, the volume-axis intercept of the end-systolic pressure–volume relation, V_o, was determined by using the quadratic formula to solve Equation 10 for ESV when ESP was set equal to zero.[11]

Because the shell subtraction model provides simultaneous estimates of both right and left ventricular volumes, it has potential applications to studies of the simultaneous responses of both ventricles to any intervention and to studies of ventricular interactions. To demonstrate this facility of the model and to document the normal differences between quantitative indexes of right and left ventricular systolic function, the same procedures described above were used to determine the simultaneous stroke work/end-diastolic volume and end-systolic pressure–volume relations of the left ventricle. Summary data are expressed as mean±1 SD.

Results

Isolated Heart Studies

The results of multiple linear regression analyses of the relations between right ventricular free wall dimensions and the volumes of both the right and left ventricles in all isolated heart studies are summarized in Table 1. When left ventricular volume was held constant, the relations between right ventricular free wall segment length (or segment area) and right ventricular volume were highly linear. As demonstrated in Figure 2, however, the linear relations between right ventricular free wall dimensions and right ventricular volume were shifted progressively upward by increments in left ventricular volume, indicating interdependence of right and left ventricular dimensions. In fact, multiple regression analyses demonstrated that the linear correlation coefficients of the relation between right ventricular free wall dimensions and left ventricular volume were remarkably similar to those found for the relations with right

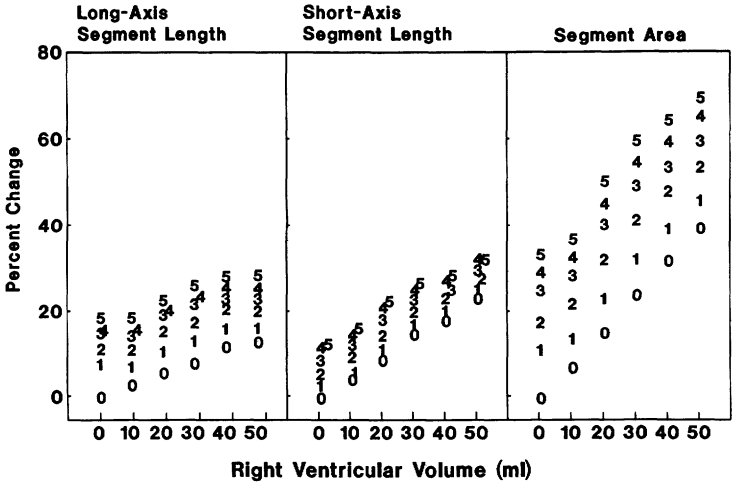

FIGURE 2. *Multiple relations between right ventricular free wall regional dimensions and right ventricular balloon volume in one representative heart when left ventricular balloon volume was increased in increments of 10 ml from 0 to 50 ml. To aid clarity, each 10-ml increment in left ventricular balloon volume is numbered from 1 to 5. Dimensional changes are expressed as percent change from control at zero right and left ventricular balloon volumes.*

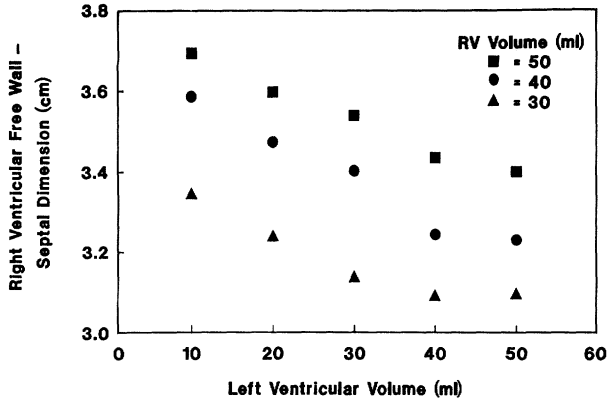

FIGURE 3. *Relations between right ventricular septal–free wall diameter and left ventricular balloon volume at three different, fixed levels of right ventricular (RV) balloon volume.*

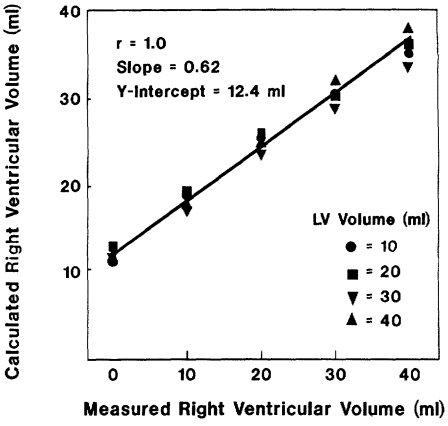

FIGURE 4. *Linear relation between calculated right ventricular volume (Equation 5) and measured (balloon) right ventricular volume. The relation was insensitive to wide variations in left ventricular (LV) balloon volume.*

ventricular volume, but the slopes of the relations with left ventricular volume were systematically lower (Table 1). For example, the average slope of the relation between right ventricular free wall segment area and left ventricular volume was 0.33, whereas the average slope of the relation with right ventricular volume was 1.03. The ratio of these slopes indicates that changes in left ventricular volume exerted approximately one third of the effect on free wall segment area as changes in right ventricular volume.

Similarly, right ventricular septal–free wall diameter was dependent on the volumes of both ventricles (Figure 3), although the effect of left ventricular volume on this dimension tended to plateau at higher volumes, perhaps reflecting the attainment of maximal rightward septal curvature. Multiple regression analyses of the right ventricular septal–free wall diameter data indicated a strong, positive linear relation with right ventricular volume ($r=0.98\pm0.01$, slope$=0.25\pm0.03$ mm/ml) and a strong but inverse linear relation with left ventricular volume ($r=-0.98\pm0.01$, slope$=-0.11\pm0.04$ mm/ml). The absolute ratio of the slopes of these two relations ($0.11/0.25=0.44$) indicates that the sensitivity of the right ventricular septal–free wall diameter to changes in left ventricular volume was 44% of that to changes in right ventricular volume.

The relation between right ventricular volume calculated with Equation 5 and right ventricular balloon volume also was highly linear (Figure 4), although the slope and intercept of the relation varied from heart to heart. Linear regression data from all 11 isolated heart studies are given in Table 2. Unlike the relation between right ventricular dimensions and volume, however, multiple regression analyses indicated that the relation between calculated and measured right ventricular volumes was independent of left ventricular volume in every dog (Figure 4). That is, at any given right ventricular balloon volume, no significant relation was observed between estimates of right ventricular volume according to Equation 5 and left ventricular balloon volume.

TABLE 2. Linear Regression of Calculated Versus Measured Right Ventricular Volume

Heart No.	Experimental preparation	Slope	*y* intercept (ml)	*r*	*p*	SEM (ml)
1	Excised	0.56	1.8	1.0	<0.001	1.5
2	Excised	0.73	2.4	0.99	<0.001	1.6
3	Excised	0.77	10.5	1.0	<0.001	4.8
4	Excised	0.92	−3.6	0.99	<0.001	2.0
5	Excised	0.85	13.3	1.0	<0.001	1.8
6	Excised	1.02	17.5	0.99	<0.001	2.0
7	Excised	0.64	36.1	0.97	<0.001	1.9
8	Excised	0.70	9.4	0.99	<0.001	2.0
9	Perfused	0.47	7.3	0.99	<0.001	0.9
10	Perfused	0.62	12.4	1.0	<0.001	0.8
11	Perfused	0.92	−4.8	0.98	<0.001	2.6
Mean		0.75	9.3	0.99		
SD		0.17	11.3	0.01		

Each regression is based on pooled data for all variations in left ventricular volume.

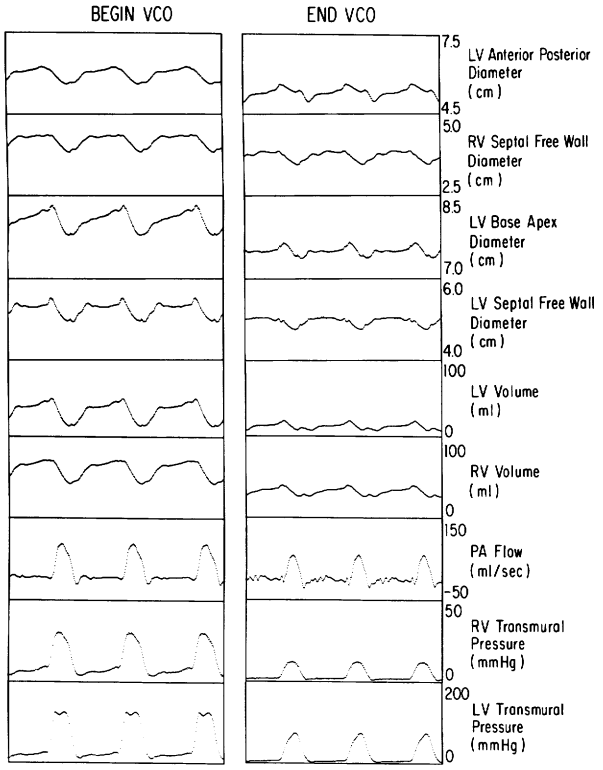

FIGURE 5. *Representative digital data obtained from one conscious dog before vena caval occlusion (BEGIN VCO) and at maximal vena caval occlusion (END VCO). LV, left ventricular; RV, right ventricular; PA, pulmonary artery.*

In Vivo Studies

Typical digital data obtained in the conscious dog under control conditions and during transient vena caval occlusion are shown in Figure 5. After the onset of vena caval occlusion, a progressive beat-to-beat reduction was observed in all four ultrasonic dimensions and in the pressures and volumes of both ventricles. After vena caval occlusion, the onset of reduction in calculated right ventricular volume preceded that of the left ventricle because of pulmonary transit delay.

The relation between calculated right ventricular stroke volume and stroke volume measured with the pulmonary artery flow probe is shown in Figure 6 for each of the four dogs studied. In each case, the relation between calculated and measured right ventricular stroke volume was highly linear, with a slope near unity.

Typical pressure–volume loops obtained from the left and right ventricles during transient vena caval occlusion are shown in Figure 7. Also shown are the corresponding stroke work/end-diastolic volume and end-systolic pressure–volume relations derived from the pressure–volume loops. Individual regression data are given in Tables 3 and 4.

The left ventricular stroke work/end-diastolic volume relation was highly linear in all cases, as has been reported previously.[3] The right ventricular stroke work/end-diastolic volume relation also was

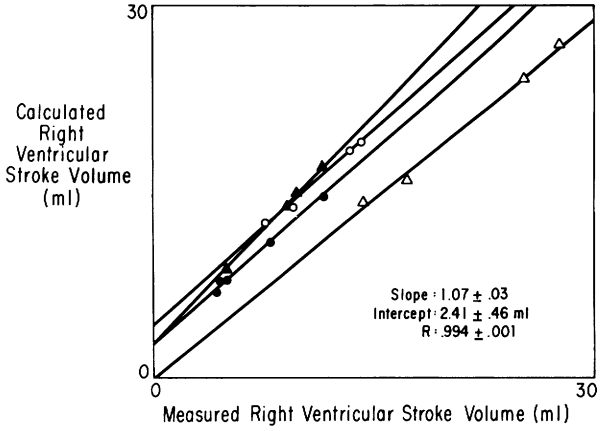

FIGURE 6. *Linear relations between calculated (right ventricular volume model) and measured (pulmonary artery flow probe) right ventricular stroke volumes in four dogs.*

linear, and parameter A_s in Equation 9 did not differ significantly from zero for either the left (0.03 ± 0.16) or right (0.01 ± 0.04) ventricle. As expected, the slope of the right ventricular stroke work/end-diastolic volume relation was much lower than that of the left ventricle.

The right ventricular end-systolic pressure–volume relation also was highly linear ($A_p=-0.01\pm0.09$), but the left ventricular end-systolic pressure–volume relation was significantly curvilinear. For the left ventricle, parameter A_p in Equation 10 was less than zero in each of the nine dogs (-0.46 ± 0.45, $p<0.02$), indicating significant concavity of the end-systolic pressure–volume relation of the left ventricle toward the volume axis (Figure 7). Nevertheless, linear correlation coefficients for the left ventricle were high in most cases, although linear extrapolation produced more negative volume-axis intercepts (Table 4). Nonlinear determinations of V_o according to the quadratic formula were consistently higher but were still negative in several cases. The latter observation reflects the inability of vena caval occlusion to produce a sufficiently low range of left ventricular volumes to permit precise extrapolation to the actual V_o, even when the quadratic formula is used.[12]

It is notable also that, at maximal vena caval occlusion, less reduction was observed in the end-systolic pressures of both ventricles than in stroke work (Figure 7). At maximal vena caval occlusion, left and right ventricular stroke work averaged $23.1\pm16.7\%$ and $19.1\pm13.4\%$ of control values, respectively, whereas the corresponding end-systolic pressures averaged $69.9\pm12.8\%$ and $56.5\pm15.3\%$ of control. Consequently, determination of the volume-axis intercepts of the stroke work/end-diastolic volume relations of both ventricles required far less extrapolation from the measured data than did determination of the volume-axis intercepts of the end-systolic pressure–volume relations.

Discussion

This report confirms previous studies demonstrating a linear relation between right ventricular free

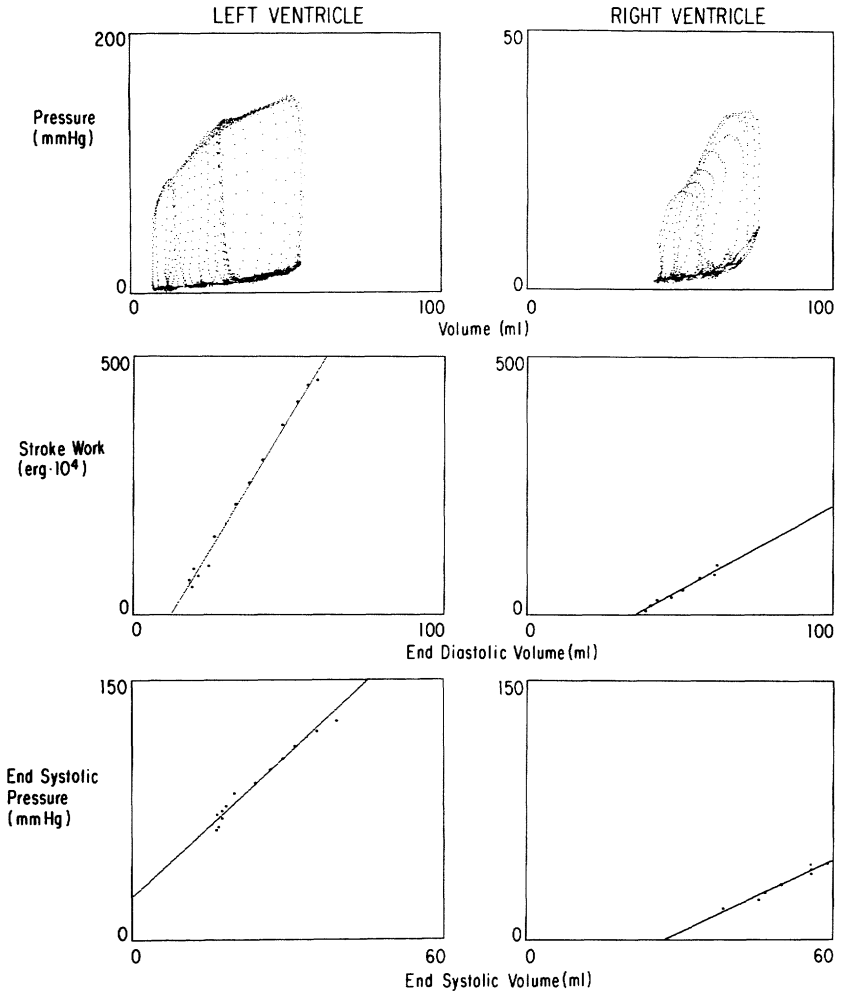

FIGURE 7. Upper panels: *Comparison of pressure–volume loops recorded from the left and right ventricles of a representative conscious dog during vena caval occlusion. Note the lower pressure scale used for the right ventricle and the less rectilinear shape of the right ventricular pressure–volume loops.* Middle panels: *Comparison of the stroke work/end-diastolic volume relations of the left and right ventricles derived from the pressure–volume loops in the upper panels. Note the highly linear nature of both relations and that the stroke work of both ventricles is close to zero at maximal vena caval occlusion. As expected, the slope of the right ventricular relation is much lower than that of the left ventricle.* Lower panels: *Comparison of the end-systolic pressure–volume relations of the left and right ventricles derived from the pressure–volume loops in the upper panels. Linear regression lines are shown. Note that the right ventricular relation is quite linear, whereas the left ventricular relation tends to be concave toward the volume axis, producing a negative volume–axis intercept with linear extrapolation. Also note a smaller reduction in end-systolic pressure than in stroke work for both ventricles during vena caval occlusion.*

wall dimensions and right ventricular volume[5,6]; in each of these studies, however, the possibility of an independent relation between right ventricular free wall dimensions and left ventricular volume was not considered. Based on the present data, it now would appear that changes in left ventricular volume significantly influence right ventricular geometry because of ventricular interdependence. As an example, an increase in left ventricular volume at a constant right ventricular volume reduces right ventricular septal–free wall diameter (Figure 3), and to accommodate the constant right ventricular volume, the dimensions

TABLE 3. Stroke Work/ End-Diastolic Volume Relations

	Left ventricle			Right ventricle		
Dog	r	M_w (erg · ml^{-1} · 10^4)	V_w (ml)	r	M_w (erg · ml^{-1} · 10^4)	V_w (ml)
1	0.98	10.9	5.7	0.99	1.5	18.9
2	0.99	10.0	8.7	0.99	2.1	17.9
3	0.99	6.9	10.6	0.99	1.3	15.0
4	0.99	12.0	5.0	0.97	2.5	2.5
5	0.99	9.6	24.1	0.98	2.8	16.5
6	0.99	14.4	6.8	0.99	2.7	39.4
7	0.99	12.7	9.4	0.99	1.4	1.4
8	0.99	9.1	4.5	0.99	1.4	37.1
9	0.99	10.0	11.8	0.98	3.3	46.7
Mean	0.99	10.6	9.6	0.99	2.1	21.7
SD	0.00	2.2	6.0	0.01	0.7	16.0

M_w, slope; V_w, volume–axis intercept.

TABLE 4. End-Systolic Pressure–Volume Relations

Dog	Left ventricle				Right ventricle		
	r	E_{ES} (mm Hg · ml^{-1})	Linear V_o (ml)	Nonlinear V_o (ml)	*r*	E_{ES} (mm Hg · ml^{-1})	V_o (ml)
1	0.86	3.6	−16.7	−5.7	0.99	1.9	17.4
2	0.97	4.0	−12.2	−2.5	0.99	1.4	6.6
3	0.99	3.8	3.1	11.4	0.99	1.4	11.1
4	0.99	4.7	−11.5	−4.2	0.96	2.1	1.5
5	0.99	5.4	15.8	20.8	0.98	1.4	−1.5
6	0.99	6.2	−8.0	−3.1	0.99	1.7	39.4
7	0.98	8.2	0.8	5.5	0.99	2.2	−3.8
8	0.98	8.6	−0.4	3.1	0.99	1.6	39.0
9	0.99	2.8	−9.0	−1.2	0.99	1.4	26.5
Mean	0.97	5.3	−4.2	2.7	0.99	1.7	15.1
SD	0.04	2.1	10.0	8.7	0.01	0.3	16.6

E_{ES}, slope; V_o, volume–axis intercept (linear extrapolation); nonlinear V_o, value derived from quadratic formula (see text).

of the right ventricular free wall increase (Figures 2 and 8). Thus, the use of free wall dimensions as indexes of right ventricular volume in the intact heart may not be entirely valid, because left ventricular volume varies significantly during the cardiac cycle. Right ventricular septal–free wall diameter also has been used as the sole index of right ventricular volume changes in studies of direct ventricular interaction.[7] The data illustrated in Figure 3 suggest that this approach also is questionable.

In contrast to measurements of regional right ventricular dimensions, the ellipsoidal shell subtraction method of determining right ventricular volume was insensitive to changes in left ventricular volume (Figure 4). Variability in the slope and intercept of the actual versus predicted right ventricular volume relation (Table 2) presumably reflects individual variation in cardiac geometry and/or alignment of the ultrasonic dimension transducers, as has been reported previously for left ventricular volume algorithms.[4]

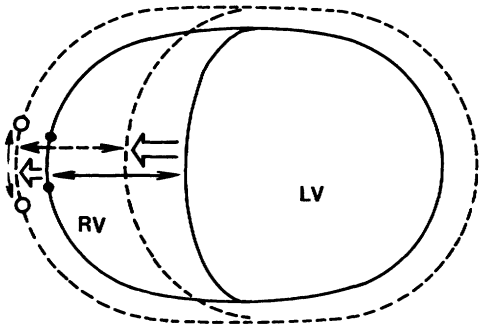

FIGURE 8. *Effects of an increment in left ventricular (LV) volume on right ventricular (RV) geometry at constant right ventricular volume. A pair of ultrasonic dimension transducers are shown as closed circles on the right ventricular free wall under control conditions (unbroken lines). With an increment in left ventricular volume (broken lines), the interventricular septum is displaced rightward, with a consequent reduction in right ventricular septal–free wall diameter. Under these conditions, the constant right ventricular volume can be accommodated only by an increase in the dimensions of the right ventricular free wall, exemplified by an increase in the segment length (open circles).*

When the right ventricular volume model was applied in vivo, dimensional estimates of right ventricular stroke volume were related in a highly linear manner to measured stroke volume, with a slope close to unity in all cases (Figure 6). The potential utility of continuous measurements of dynamic right ventricular volume was illustrated by using the volume algorithm to generate right ventricular pressure–volume loops during vena caval occlusion. Right ventricular stroke work/end-diastolic volume and end-systolic pressure–volume relations derived from those pressure–volume loops were qualitatively similar to relations obtained for the left ventricle and provided quantitative linear indexes of right ventricular systolic function. In fact, the end-systolic pressure–volume relation of the right ventricle was found to be more strictly linear than that of the left ventricle.

The shell subtraction model provides the only method described to date for recording continuously instantaneous right ventricular volume in the conscious state. Only two other methods that provide estimates of right ventricular volume with a reasonably high sampling frequency in vivo have been described.[13,14] Because both of these methods depend on biplane cineradiography of surgically implanted radiopaque markers, however, they have been applied only in anesthetized dogs. One of these methods, described by Schwiep and colleagues,[14] has the advantage of not relying on any geometric assumptions concerning right ventricular shape, but it necessitates implantation of 18 radiopaque markers throughout the right ventricular shell. In addition, the sampling frequency of this technique is limited to 60 Hz by the cineradiographic frame rate. In contrast, the sampling frequency of the shell subtraction method is limited only by the analog-to-digital conversion rate (200 Hz in the present study), because the

analog dimensional data from which right ventricular volume is calculated are recorded continuously.

Several limitations of the present study must be considered. The initial validation of the shell subtraction model in isolated hearts was performed by comparing calculated right ventricular volume with the fluid volume contained in an intraventricular balloon,[15] but the balloon technique has not been independently validated for the right ventricle. It is conceivable that a balloon might adapt less well to the more complex internal surface of the right ventricle. The good correlation observed in vivo, however, between calculated and measured stroke volumes provides independent evidence of the shell subtraction model's accuracy as an index of right ventricular volume.

Nevertheless, there is a discrepancy between the validation data obtained in vivo and the data obtained from isolated hearts. In most isolated hearts, the slope of the relation between calculated and measured right ventricular volumes was less than 1.0 (Figure 4 and Table 2). Consequently, if the relation between calculated and measured volumes remained constant throughout ejection, it would be predicted from the isolated heart data that the shell subtraction model would underestimate right ventricular stroke volume. In vivo, however, the slope of the relation between calculated and measured stroke volumes slightly exceeded 1.0, and the intercept with the ordinate was slightly positive in most cases (Figure 6), indicating that the model tended to overestimate stroke volume. One possible explanation for these different observations is that the relation between calculated and measured right ventricular volume in vivo slightly exceeds 1.0. A more plausible explanation, however, is that the altered relation between calculated and actual right ventricular volume during ejection is due to a change in right ventricular shape, with a consequent underestimation of the volume at end-ejection relative to the volume estimated at the onset of ejection. The net consequence of this shape change, however, is that the shell subtraction model provides a more accurate estimate of stroke volume than of absolute volume and is best regarded as a volume index. The same may be said of most left ventricular volume algorithms.[1-4]

Finally, it must be noted that the need to measure the volume of the right ventricular free wall to calculate right ventricular chamber volume limits current application of the shell subtraction model to longitudinal studies of animals developing cardiac enlargement or hypertrophy. The recent development of echocardiographic methods[16] to measure left ventricular wall volume facilitates the application of the left ventricular ellipsoidal volume algorithm (Equation 3) to longitudinal closed-chest studies. Development of a similar echocardiographic means of measuring right ventricular free wall volume in vivo may solve this problem for the right ventricle as well.

In conclusion, the observations of this study provide a fundamental basis for future investigation of right ventricular function and ventricular interaction in the intact heart. An accurate method for measuring the dynamic volumes of both ventricles simultaneously should enhance the knowledge of integrated cardiac performance and facilitate an improved understanding of circulatory dynamics under normal and pathological conditions.

References

1. Rankin JS, McHale PA, Arentze CE, Ling O, Greenfield JC Jr, Anerson RW: The three-dimensional dynamic geometry of the left ventricle in the conscious dog. *Circ Res* 1976;39: 304–313
2. Olsen CO, Tyson GS, Maier GW, Spratt JA, Davis JW, Rankin JS: Dynamic ventricular interaction in the conscious dog. *Circ Res* 1983;52:85–104
3. Glower DD, Spratt JA, Snow ND, Kabas JS, Davis JW, Olsen CO, Tyson GS, Sabiston DC Jr, Rankin JS: Linearity of the Frank-Starling relationship in the intact heart: The concept of preload recruitable stroke work. *Circulation* 1985;71:994–1009
4. Sodums MT, Badke FR, Starling MR, Little WC, O'Rourke RA: Evaluation of left ventricular contractile performance utilizing end-systolic pressure-volume relations in conscious dogs. *Circ Res* 1984;54:731–739
5. Hamm DP, Everson CT, Freedman BM, Pellom GL, Christian C, Wechsler AS: The passive right ventricular volume-dimension relationship in the isolated canine heart. *Surg Forum* 1984;35:266–268
6. Morris JJ III, Pellom GL, Hamm DP, Everson CT, Wechsler AS: Dynamic right ventricular dimension: Relation to chamber volume during the cardiac cycle. *J Thorac Cardiovasc Surg* 1986;91:879–887
7. Slinker BK, Glantz SA: End-systolic and end-diastolic ventricular interaction. *Am J Physiol* 1986;251:H1062–H1075
8. Feneley MP, Olsen CO, Glower DD, Rankin JS: Effect of acutely increased right ventricular afterload on work output from the left ventricle in conscious dogs. *Circ Res* 1989;65: 135–145
9. Tyson GS Jr, Maier GW, Olsen CO, Davis JW, Rankin JS: Pericardial influences on ventricular filling in the conscious dog: An analysis based on pericardial pressure. *Circ Res* 1984;54:173–184
10. Olsen CO, Tyson GS, Maier GW, Davis JW, Rankin JS: Diminished stroke volume during inspiration: A reverse thoracic pump. *Circulation* 1985;72:668–679
11. Burkhoff D, Sugura S, Yue DT, Sagawa K: Contractility-dependent curvilinearity of end-systolic pressure-volume relations. *Am J Physiol* 1987;252:H1218–H1227
12. Kass DA, Beyar R, Lankford E, Heard M, Maughan WL, Sagawa K: Influence of contractile state on curvilinearity of in situ end-systolic pressure-volume relations. *Circulation* 1989; 79:167–178
13. Santamore WP, Carey R, Goodrich D, Bove AA: Measurement of left and right ventricular volume from implanted radiopaque markers. *Am J Physiol* 1981;240:H896–H900
14. Schwiep F, Cassidy SS, Ramanathan M, Johnson RL Jr: Rapid in vivo determinations of instantaneous right ventricular pressure and volume in dogs. *Am J Physiol* 1988;254:H622–H630
15. Suga H, Sagawa K: Accuracy of ventricular lumen volume measurement by intraventricular balloon method. *Am J Physiol* 1979;236:H506–H507
16. Feneley MP, Gaynor JW, Maier GW, Gall SA Jr, Kisslo JA, Rankin JS: In vivo estimation of left ventricular wall volume in volume-overloaded canine hearts. *Am J Physiol* 1988;255: H1399–H1404

KEY WORDS • right ventricle • ventricular interaction • ventricular function